Observed perturbations of the velocity distribution of interstellar hydrogen atoms in the solar system with Prognoz Lyman-alpha measurements

Rosine Lallement, Jean-Loup Bertaux, V. G. Kurt, E. N. Mironova

Astron. Astrophys. 140, 243–250 (1984)

ASTRONOMY AND ASTROPHYSICS

Observed perturbations of the velocity distribution of interstellar hydrogen atoms in the solar system with Prognoz Lyman-alpha measurements

R. Lallement[1], J.L. Bertaux[1], V.G. Kurt[2], and E.N. Mironova[2]

[1] Service d'Aéronomie du CNRS, F-91370 Verrières-le-Buisson, France
[2] Space Research Institute, Academy of Sciences of USSR, 84/32 88 Profsoyouznaia, SU-117810 Moscow, USSR

Received March 29, accepted July 12, 1984

Summary. Observations of the interplanetary Lyman α emission made at five different places in the solar system with high apogee satellites Prognoz 5 and Prognoz 6 are reported. This Ly α emission is the result of resonance scattering of solar photons by H atoms of the Local Interstellar Medium flowing in the solar system at the velocity $-V_w$ and the spectral profile is an image of the velocity distribution of the atoms. A hydrogen absorption cell was used to analyze the spectral profile, the variation of Doppler shift with looking direction providing its spectral scanning. A purely geometrical method, described in detail in Bertaux and Lallement (this issue), was applied to analyze the data. A first estimate of the LISM temperature is derived, $T \simeq 8000$ K, and also an approximate location of V_w in fair agreement with previous measurements. In addition, it is shown for the first time that when averaged along a line of sight both the bulk velocity V and the thermal velocity spread of H atoms (measured by an effective temperature T_e), are changing with position in the solar system. This is a confirmation of the previously predicted effects of solar gravitation (when unbalanced by solar Lα radiation pressure) and ionization of H atoms by solar wind and EUV radiation. The apparent heating effect is larger near the downwind direction ($-V_w$). The observed variation of the heating effect is of 3000 K, and is independent of the existence of a potential galactic background in the vicinity of the Lyα wavelength. An upper limit of this background is found to be 15 Rayleigh. The observed variation of T_e with the angle with the upwind direction V_w is larger than predicted by a theoretical model of Wu and Judge (1980).

Key words: interstellar medium – interstellar hydrogen – interplanetary hydrogen – interplanetary Lyman α

1. Introduction

The Sun is moving with respect to the nearby stars with a velocity of 20 km s^{-1} in the direction of the Apex, $\alpha = 271°$ and $\delta = 30°$ (celestial coordinates). As the lights of a car illuminate the water droplets when driving in the fog, the Sun illuminates the Hydrogen and Helium atoms of the interstellar medium which it travels through. As a result, the sun and the whole solar system are embedded in a glow of the resonance lines of hydrogen (H Lyman α (121.6 nm) and helium (58.4 nm).

The detailed study of this glow allows us to probe the Local Interstellar Medium, LISM. The denser the LISM, the brighter the glow, and the intensity at Lyman α of this interplanetary glow is related to the density "at infinity" of the LISM (when not yet perturbed by the sun).

Since the solar H Ly α line is very wide all interstellar H atoms approaching the solar system are illuminated by the Sun regardless of the Doppler shift; with the Doppler effect, the scattered Ly α emission has a spectral profile which is exactly the image of the velocity distribution of the hydrogen atoms at the place of the emission. Therefore, if the scattered Ly α emission profile can be measured very accurately, the bulk velocity of the H atoms can be derived from the global Doppler shift of the line, and the temperature T can be derived from the linewidth.

In a companion paper (Bertaux and Lallement, this issue), referred to as paper 1 from now on, the use of a hydrogen absorption cell associated to a Lyα photometer has been fully described to study the line profile of the Ly α interplanetary emission from H atoms of the LISM flowing into the solar system. The principle is that, looking at various directions in the sky, the absorption of the cell (used at a fixed optical thickness $\tau \simeq 10$) is modulated by the Doppler shift between the observer and the emitting gas. An angular scan provides a spectral scan of the emission line, and the method is called the Doppler Angular Spectral Scanning method.

In paper 1, the simple case in which the velocity distribution of H atoms is not modified by the sun was completely analyzed. In this case, referred to also as the uniform gaussian case, there is a uniform flow of H in the solar system, and the same gaussian spectral shape is observed in all directions; the Doppler shift $\Delta\lambda_D$ of the line is related to the angle α between the line of sight U and the relative velocity vector $V_R = V_s + V_w$:

$$\Delta\lambda_D = \frac{\lambda_0}{c} V_R \cos(V_R, U) = \frac{\lambda_0}{c} V_R \cos\alpha = \frac{\lambda_0}{c} V_D. \quad (1)$$

V_w is the velocity vector of the solar system through the LISM, V_s is the velocity of the observer in the solar system, V_R is the velocity of the observer relative to H atoms of the LISM, and c is the velocity of light.

The absorbing effect of the hydrogen absorption cell is measured by the reduction factor $R = I_{ON}/I_{OFF}$, the ratio of the measured intensity I_{ON} when the cell is activated, to the intensity I_{OFF} when the cell is not activated.

Send offprint requests to: R. Lallement

The results of the theoretical study of Paper 1 are summarized below, for the uniform gaussian case:

– the distribution of R on the celestial sphere has a symmetry of revolution about the vector $V_R = V_s + V_w$. It looks like a crunched apple or a peanut respectively for large and low values of V_R. Minimum values R_{min} of the reduction factor are distributed along a great circle of the celestial sphere (the Zero Doppler Shift Circle), perpendicular to V_R.

– The value of R_{min} directly determines the temperature (if there is no superimposed galactic background, not affected by the absorption cell).

– A geometrical method was established to retrieve the vector V_w from three sets of R measurements in three different planes. This purely geometrical method does not require any modelling, and is still valid in the presence of some superimposed galactic background.

If more than three sets of measurements are used and give inconsistent results for the vector V_w when they are analyzed by groups of three, it is clearly an indication that the reality departs from the uniform gaussian case. The velocity distribution of H atoms may be modified in the theory by the following effects:

– the unbalance between solar gravitation F_g and the Ly α solar radiation pressure F_r, described by the parameter $\mu = F_r/F_g$ (Fahr, 1974; Fahr, 1978) provides a mechanical effect which bends individual trajectories into hyperbolae.

– The solar ionization is more effective on slow atoms than on fast atoms (Wu and Judge, 1979; Lallement, 1983).

– Heating by solar corpuscular emissions should be only a minor effect (Holzer, 1977; Wu and Judge, 1978; Kunc et al., 1983).

These effects can be modelled with expensive computer codes. Wu and Judge (1980) computed the exact velocity distribution in a particular case relevant to an early estimate of the LISM temperature with Prognoz 5 (Bertaux et al., 1977). In order to compare to Prognoz 5 line width measurements, they had to compute line profiles, which are the velocity distribution of H atoms, projected along the line of sight, with r^{-2} weighting function to account for the solar flux decrease. The computed Lα profile was looking very much a gaussian, and Wu and Judge could define and "effective temperature" T_e defining the "best fit" gaussian to the Lα profile. They computed that, for the PROGNOZ particular geometry of observation, the velocity distribution (projected, integrated and weighted along the line of sight) was widened and the effective temperature T_e was greater than the temperature T at infinity of the LISM by $\Delta T \simeq 1{,}800$ K. However, it should be noted that the widening of the Lα profile may reflect either a "local" heating effect, or a bulk velocity variation along the line of sight, or a combination of both effects. Since the temperature is a locally defined quantity, it may be slightly abusive to talk of an "effective temperature", which refers here to a quantity integrated along a line of sight. Still, we will from now on follow the usage of Wu and Judge (1980) of this "effective temperature" concept, designating in fact the width of a gaussian fitting a Lα profile. In their study, Wu and Judge had to assume a certain value of the Lyα radiation pressure parameter, $\mu = 0.75$, without knowing the actual value.

In fact, a value of $\mu = 1.0$ is as much likely as the value $\mu = 0.75$, in which case all atoms are travelling uniformly along straight lines. If, in addition, the ionization is weak, the velocity distribution is not substantially modified and the uniform gaussian case is valid.

Up to now, there has been only one observation suggesting that indeed the H velocity distribution is modified by the Sun environment, reported by Cazes and Emerich (1977). With the French satellite D2-A, deeply imbedded in the geocorona at 600 km of altitude, they could use the geocoronal hydrogen as a sort of absorption cell to analyze the interplanetary emission. However, their measurements suffer by the same token of a heavy geocoronal contamination.

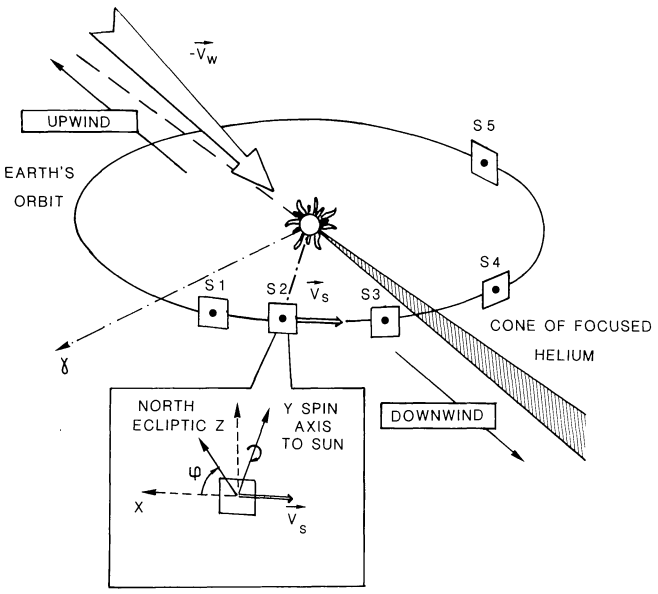

Fig. 1. Geometrical configuration of the Prognoz measurements discussed in the present paper. The positions of the earth corresponding to the five seances of observations, noted S_1 to S_5 are shown along the earth's orbit. The ecliptic longitudes are given in Table 1. The spin axis of the Prognoz satellites were pointed to the Sun and thus the scan planes are normal to the ecliptic plane and contain the earth's velocity, vector V_s. The spin angle ϕ is measured from the opposite direction $-V_s$. The North ecliptic direction corresponds to $\phi = 90°$

In the present paper, we report observations made with a Ly α photometer placed on board two Soviet satellites, Prognoz 5 and Prognoz 6, in 1976 and 1977, at a distance of $\simeq 200{,}000$ km, where geocoronal contamination is absent.

The data provide a Doppler angular spectral scanning in five planes, and are analyzed with the geometrical method described in paper 1. Using the assumption of a uniform gaussian case (no modification of the velocity distribution), a first estimate of T and V_w is obtained. However, there are systematic deviations which show clearly that indeed the velocity distribution is modified. The case of a possible galactic background is discussed and shown that it cannot account for the observed deviations.

A complete analysis of the data, which would simultaneously give an accurate estimate of T and V_w, and an estimate of μ and the solar ionization do require a complex modelling, which is presently in progress and will be published later. This sophisticated analysis will conclude an effort lasting since twelve years, started in 1972 in Tbilissi when it was decided between French and Soviet scientists to study the interstellar/interplanetary emission with the technique of Doppler Angular Spectral Scanning method.

2. Observations of Prognoz 5 and Prognoz 6

Prognoz 5 data were collected from December 1976 to April 1977 and Prognoz 6 data were collected from September 1977 to January 1978. Both spacecrafts were orbiting the Earth on a very eccentric orbit, with a period of 4 days and an apogee distance of 200,000 km.

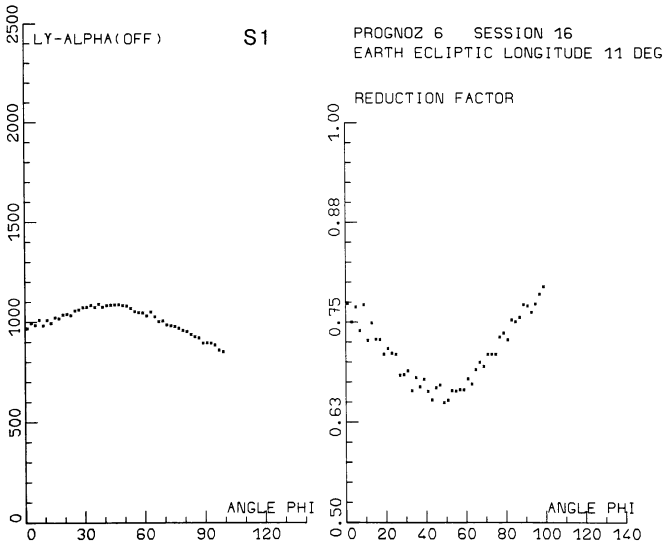

Fig. 2

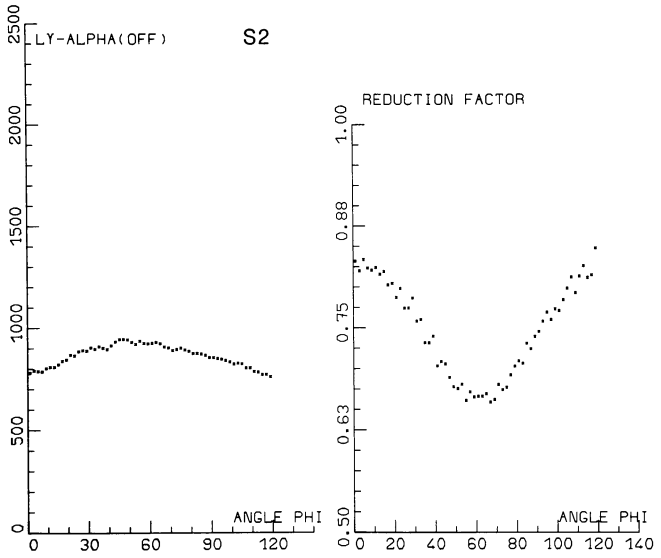

Fig. 3

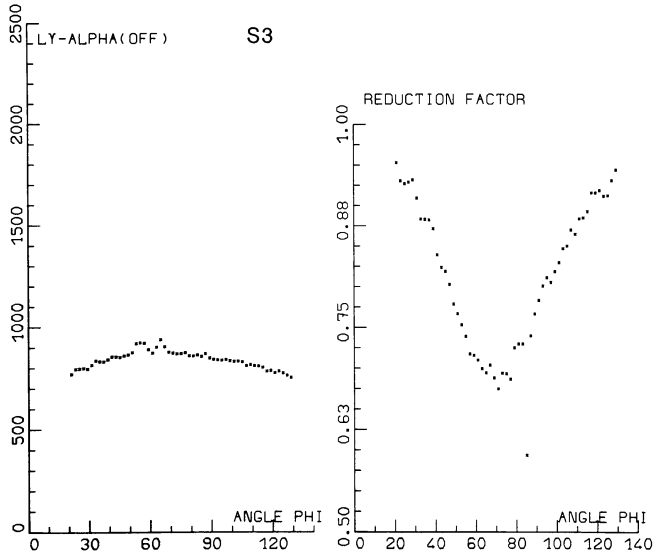

Fig. 4

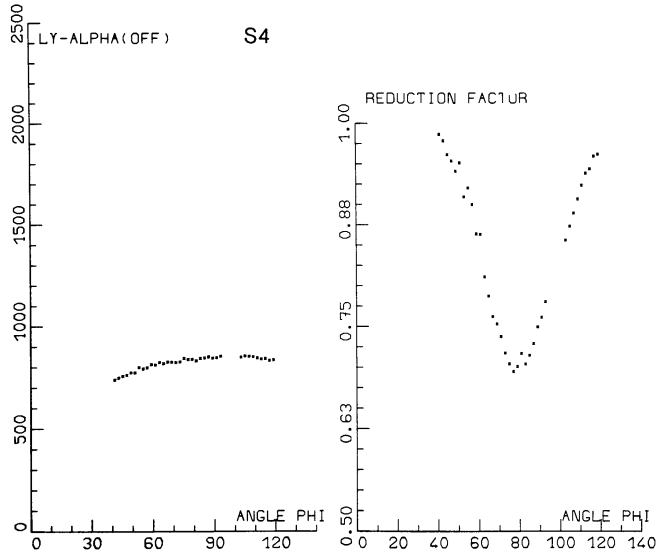

Fig. 5

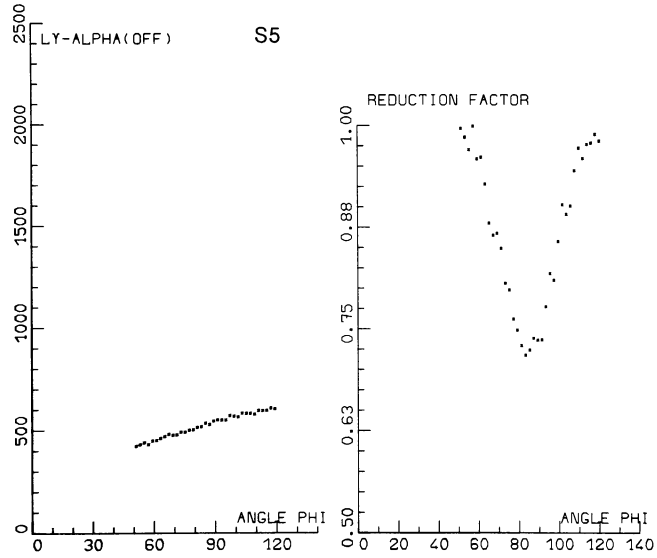

Fig. 6

Figs. 2–6. For each seance are given both the intensity I_{OFF} (signal recorded with cell OFF) and the reduction factor R, which is the fraction of the signal which is not absorbed by the cell ($R = I_{ON}/I_{OFF}$). These two results are plotted as a function of the spin angle ϕ. The absorption troughs corresponding to positive ecliptic latitudes are only shown. Intensities are given in counts s^{-1}. A first estimate of the calibration factor yielded a sensitivity of 3.7 counts Rayleigh^{-1} s^{-1} for Prognoz 6 and 2.1 counts Rayleigh^{-1} s^{-1} for Prognoz 5. Figs. 2–6 correspond respectively with the S_1, S_2, S_3, S_4, S_5 number of observation

Table 1

Observation	S_1	S_2	S_3	S_4	S_5
Earth's ecliptic longitude (degrees)	11	29	58	85	151
Record duration (hours)	24	30	36	36	30
Optical thickness of the cell τ	10	10	10	10	8
Direction of maximum absorption ϕ_m (degrees)	47,0	62,1	70,0	79,0	84,8
Minimum value of reduction factor	0.659	0.661	0.684	0.692	0.715
Corresponding apparent temperature (Kelvin)	8,450	8,550	10,000	10,500	11,300
Projection V_{pt} of the relative velocity vector on the scanning plane (km s^{-1})	11.3	14.3	21.9	34.3	46.4
Component normal to ecliptic of the relative velocity V_{wz} (km s^{-1})	7.5	6.7	7.3	6.7	4.0
Angel θ between the direction of maximum absorption and the upwind direction (degrees)	46.9	64.9	78.8	86.1	89.1

Here we analyze the data collected during five periods of measurements referred as S_1, S_2, S_3, S_4, S_5 each lasting from 24 to 36 h. The corresponding five positions of the Earth in the solar system are shown on Fig. 1 and are distributed along half of the Earth's orbit. Thus, the measurements are covering 5 different planes perpendicular to the Sun-Earth line. Each plane corresponds to a different velocity of the spacecraft in respect to the gas. The velocity of the spacecraft relative to the solar system is very close to V_T, the earth's velocity, since data were recorded very near the apogee, where the orbital velocity is quite small.

The distribution in the five planes of the measured intensity $I(\phi)$ are presented on Figs. 2 to 6 as a function of angle ϕ between the vector $-V_T$ and the direction of sight, with $\phi = 90°$ for the direction of the North ecliptic pole and $\phi = 270°$ for the South ecliptic pole.

Photons were counted during 1.03 s every 10.3 s, alternately with the absorption cell not activated, for the measurement of $I_O = I_{OFF}$, and with the cell activated for the measurement of the reduced intensity I_{ON}. The curve $I(\phi)$ corresponds to I_{OFF}, whereas the curve $R(\phi)$ corresponds to $R = I_{ON}/I_{OFF}$.

The size of the field-of-view is $1°.3 \times 3°$, the length being in the scan plane. Since the spacecraft is spin stabilized with a rotation rate of $\simeq 3°\,s^{-1}$, the dynamic FOV is enlarged to about $\simeq 6°$ in the direction of the scan motion. An optical filter deposited on the exit window of the H cell defines a bandwidth of $\simeq 100$ Å centered at Ly α (1216 Å).

For a typical period length of 24 h, more than 4200 data points of each types (ON and OFF) were accumulated and averaged into bins of the spin angle ϕ of size $\Delta\phi = 2°$, and each point plotted on Figs. 2 to 6 correspond to an average of about 25 to 30 individual measurements, the counting rate being of a few hundreds per second. A preliminary estimate of the calibration factor using several bright UV stars indicates a sensitivity of about 3.7 counts s^{-1} Rayleigh^{-1} for Prognoz 6 and 2.1 counts s^{-1} Rayleigh^{-1} for Prognoz 5. Here we have shown the data restricted to the hemisphere with positive ecliptic latitudes, because measurements in the south ecliptic directions were slightly contamined by geocoronal Lα emission. The optical thicknesses used were $\tau = 8$ and $\tau = 10$ respectively for Prognoz 5 and Prognoz 6.

It is clear in Figs. 2 to 6 that the angular width of the absorption region changes along the earth's orbit, as expected from the discussion in Sects. 3 and 4 of Paper 1. During observation S_1, corresponding to an ecliptic longitude of the earth $\lambda_e = 11°$, the absorption trough is very wide (this means that the ecliptic components of the velocities of the gas and of the earth have similar directions, and that the relative velocity V_R is small) whereas for observation S_5 ($\lambda_e = 151°$) the angular size of the absorption region is quite narrow (this means the ecliptic components of the two velocities are not far from being opposite). We can deduce that the ecliptic longitude of $-V_w$ is around 80°, an intermediate value between 11° and 151°. This defines approximately the downwind position in the ecliptic coordinates system. The direction of maximum absorption also varies as a result of the composition of gas velocity with the different positions of V_T. Since the composition of V_w and V_T has a strong effect, it shows that the value of the gas velocity V_w is not negligible, and of the same order of magnitude as the $V_T = 30$ km s^{-1} of the earth orbital motion.

Applying now the first step of the method described in Sect. 4 of Paper 1 we use the minimum values of $R(R_{min})$ to derive the gas temperature (Fig. 5 of Paper 1). Instead of the single value expected in the case of the uniform gaussian gas, the values of R_{min} are not identical for all the five observations and yield temperatures ranging from 8400 ± 500 K to $11{,}300 \pm 500$ K. The differences observed are quite larger than the uncertainties of the measurements (Table 1). This fact, which indicates a systematic departure from the uniform gaussian case will be later discussed further.

Assuming for the time being that the measured temperatures are reflecting only changes in the size of the velocity distribution of the gas, but that the bulk velocity is still constant and uniform, we now continue with the determination of V_w according to the first procedure of paper 1. For each absorption profile we use the corresponding temperature and a sample of values of $R(\phi)$ on the two sides of the minimum found at ϕ_{min} to derive the projected relative velocity *Vpt* (see Sect. 4, Paper 1). The results of the calculation are presented in Table 1. The construction of the projection V_{we} of V_w on the ecliptic plane is shown, in Fig. 7. Only the "good" choice for A' are represented; they lie in the North Ecliptic hemisphere. All lines $O'A'$ should intersect at a single point, but they do not, as it is seen in Fig. 7. However, they intersect in a small region which allows a first approximation of V_w in the following range:

$\lambda_W = 253°$ to $281°$
$\beta_W = 9°$ to $24°$ in ecliptic coordinates.

The magnitude of the velocity is found in the range $V_w = 17.5$ to 25.4 km s^{-1}.

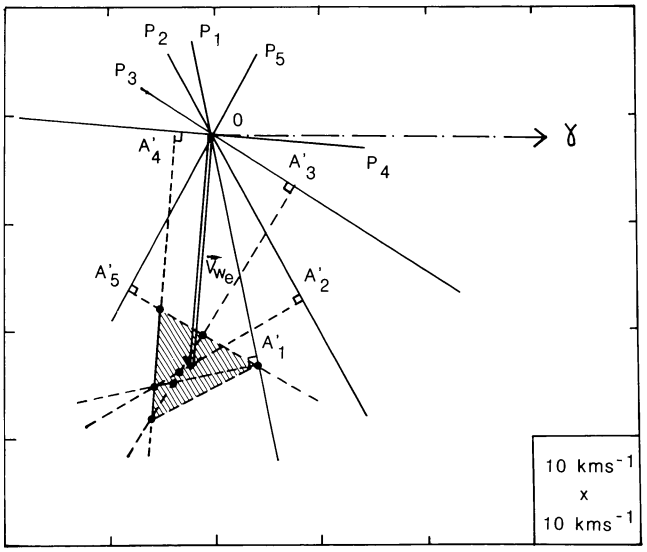

Fig. 7. A determination of the velocity vector V_w is obtained with the first geometrical method of paper 1, which assumes non contribution of the galactic background. The plane of the figure is parallel to the ecliptic plane, and 0 is the origin of the velocity space. The line 0γ indicates the axis of reference. Each scan plane crosses the plane of the figure along a line P_i. The projections A_i' on P_i lines of the ecliptic component V_{we} of V_w are determined, by using the minimum value R_{min} of the reduction factor and a set of R values around the minimum. (Fig. 10, 11, 12 of paper 1.) The calculation gives at the same time the component V_{wz} normal to ecliptic plane. The extremity of V_{we} should be at the common intersection of the perpendicular to P_i at point A_i' (dashed lines). For location of the extremety the obtained hatched area has been used associated with the components V_{wz} (normal to ecliptic) presented in Table 1 to give the limiting values for V_w, λ, β

There are three sources of uncertainties on the measurements. Averaging the results on a full day period may introduce a change of about 1° in the directions of sight. The departures from the ideal geometry (a scan plane perpendicular to the Sun) are less than 2° in all five seances of observations. There is also a smoothing effect of the curves $R(\phi)$ since the field-of-view is of the order of 4°. However, all these minor uncertainties cannot explain the large spread of $\simeq 25°$ in the longitudes found for V_w. The Doppler angular scanning method, applied to the present set of measurements, indicates without ambiguity a departure from the uniform gaussian case, which however, could be due to some additional galactic emission, as discussed in the next section.

3. Influence of a galactic emission

Since we know approximately the velocity vector V_w we can observe that from S_1 to S_5 periods the maximum absorption direction evolves from a direction at about 50 degrees from the upwind direction (V_w) to a direction approaching more closely the downwind region ($-V_w$). Thus, as it is seen in Table 1, there is a clear systematic effect of increase of the apparent temperature T_e from upwind to downwind directions. The most likely explanation is that it reflects an intrinsic change of the velocity distribution of the gas when it is flowing through the solar system, under the influence of radiation pressure, gravitation and solar ionization. However, a completely different explanation has to be examined: the presence of some galactic background could be an explanation for the incomplete adjustment of data to the uniform gaussian case. In fact a significant galactic intensity is not really expected; a theoretical study of Thomas and Blamont (1976) concludes that the background level should be less than 10 Rayleigh while the interplanetary signal is more than 120 Rayleigh. But there are some reasons to deal with the background problem. First even a low value of 10 Rayleigh modifies the reduction factor, yielding a temperature error of the order of 1000 K. The second reason is that the presence of a background will increase the apparent temperature T_e more in the directions of low interplanetary emissions, which correspond also to the downwind directions, and that is exactly what is observed. Thus it is necessary to use a method of analysis able to discriminate the effects of the galactic background from the changes in interplanetary Lyα profiles induced by the solar environment.

Such a method was also described in Sect. 5 of Paper 1. Instead of using the measured apparent temperature, it makes use only of the position ϕ_m where the reduction factor is minimum (where the absorption effect of the cell is maximum). It was shown in Paper 1 that these positions are very little affected by the possible presence of a galactic background. Therefore, as it is shown in Fig. 13 of Paper 1 the extremity of V_w must be in a plane π, perpendicular to the scan plane P and to the direction ϕ_m, displaced from the origin of coordinates by the vector $-V_T$(all scan planes are transferred by translation to the origin of axis of the velocity space, in the ecliptic coordinates system). Three different planes π intersect each other at one point, which must be the extremity of vector V_w. Two planes intersect along a line Δ. For the five observations, we have determined geometrically the 10 lines Δ, each line corresponding to a couple of planes. The projections of the 10 lines Δ on the ecliptic plane are represented in Fig. 8. The hatched area represents the domain which contains the extremity of the ecliptic component of V_w. The results on the normal component are given in Table 1. They are obtained from a construction identical to the construction presented in Fig. 8 but for a plane normal to the ecliptic plane. Finally we obtain the following determination of V_w

$\lambda_w = 247° - 299°$

$\beta_w = 6° - 19°$

$V_w = 21.5 - 29\ \mathrm{km\,s^{-1}}$.

The uncertainties are not reduced with respect to the preceding determination and they are even slightly greater. The fact that all Δ lines do not intersect at the same point indicates again a departure from the uniform gaussian case. But this time, a possible galactic background no longer can be invoked to explain this departure, since the position of planes are independent of the presence of such a background. Therefore it can be concluded that indeed the observations prove that the velocity distribution of H atoms is modified by the solar environment. Since the position of ϕ_m do not depend on the effective temperature T_e, modified from T by the solar environment, the inability to find a unique vector V_w indicates that the bulk velocity V of H atoms observed at various places in the solar system is different, an effect predicted when $\mu \neq 1$ and the ionization are taken into account.

Still, there might be the additional problem of a potential galactic background, which could affect the effective temperature measurements. In order to study this effect, the total intensities measured in directions of maximum absorption are now examined. It is assumed that the intensity I_g of a potential galactic background is uniform in the field of about $60° \times 20°$ around the north ecliptic pole, which contains the relevant directions of sight. Thus the measured variations of the intensity I_m are attributed to the interplanetary signal alone, I_0. When the cell is not activated, the measurement intensity is $I_m = I_0 + I_g$, whereas when it is

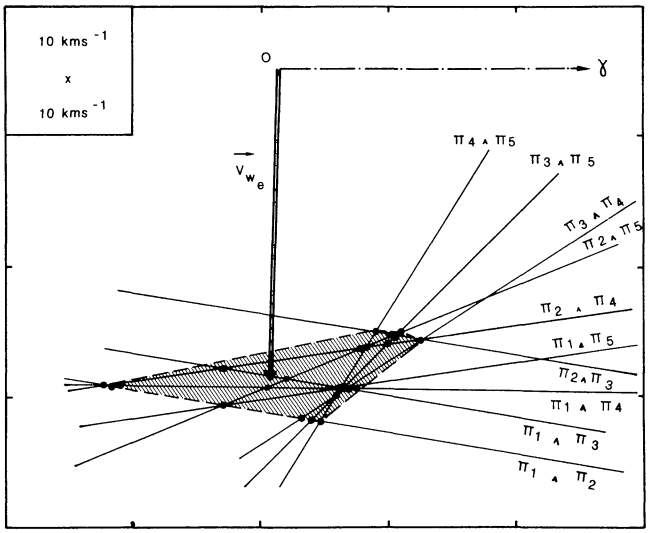

Fig. 8. The result of the second geometrical method of paper 1 to determine V_w is illustrated. This method is working even if a galactic background contribution to the signal is present. Every line noted π_i, π_j is the projection on the plane of the figure (parallel to the ecliptic) of the intersection of the two plane π_i and π_j. Each plane π contains the extremity of V_w (Fig. 13 of Paper 1). Thus this extremity should be at a common intersection of the 10 lines obtained. The hatched area has been taken as the location of the extremity. A similar construction, but projected on a plane normal to the ecliptic has been made which gave an interval for the V_{wz} component (normal to ecliptic). The assembled results have been used for the limiting values of λ, β and V_w. The fact that all planes do not cross each other at the same point means that the bulk velocities V_i of H atoms observed during the five seances are not equal to V_w, and are changing from place to place, due to the action of the solar environment

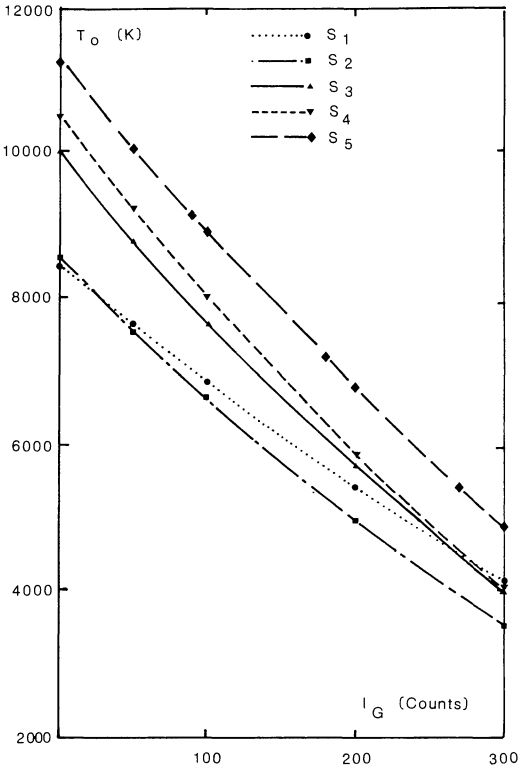

Fig. 9. A measured value R_m of the reduction factor when it reaches its minimum value $R_{\min}$ along a scan corresponds to a gaussian line with an effective temperature T_e which depends on a hypothetical galactic contribution I_g. For the five values of $R_{\min}$ measured at points S_1 to S_5, the curves T_e have been calculated for various values of the background in counts, up to 300. According to a calibration with several bright UV stars, a value of 300 counts corresponds to 80 Rayleigh (correspondence between the Prognoz 5 and 6 values has been made using the two measured sensitivities in order to present the results of calculations for S_5 on the same graph). There is no particular value of I_g which would yield a better agreement between the five measurements of T_e. The scattering of T_e measurements is real, and can be attributed to the modification of velocity distribution of H atoms by the solar environment

activated, it becomes $I_m = R_0 I_0 + I_g$, R_0 being the reduction factor applied to the sole interplanetary Ly α emission with no Doppler shift. The very wide possible galactic background is not affected by the narrow absorption feature of the H cell ($\simeq 0.03$Å, Paper 1). The measured reduction factor $R_{\min}$ is related to R_0 by:

$$R_{\min} = \frac{R_0 I_0 + I_g}{I_0 + I_g} \tag{2}$$

From this relation we can derive for an assumed value of the background I_g what would be the corresponding temperature of the emitting gas using the ratio I_0/I_g and the measured reduction factor R_m. If we assume that the velocity distribution of the gas is uniform and that changes in apparent temperature are only due to the background contributions to the signal, it should be possible to find a single value of I_g yielding the same temperature T_0 for all observations.

With the help of Fig. 5 of Paper 1 giving the relationship between the temperature T and the reduction factor $R_{\min}$, temperatures were calculated as a function of an assumed value of I_g, using (2) and the measured values $R_{\min}$ for the five observations. The five temperature curves are plotted on Fig. 9 as a function of I_g. There is no value of I_g for which the span of temperature for the five seances is significantly reduced from the span of about 3000 K found for $I_g = 0$. If there were, in addition to a background I_g, a perturbation by the solar environment of the velocity distribution, there would be a natural span of the temperatures, added to the artificial span of the apparent temperatures due to the galactic background. The fact that, in Fig. 9, the total temperature span is more or less constant, whatever is I_g, is an indication that I_g is probably very weak. (The regular and very slight diminution of the span is only due to the decrease of the sensitivity of the absorption rate with decreasing temperature.)

A method to determine the galactic background was indicated in Sect. 5 of Paper 1, which uses a comparison between the total measured emission I_m and the absorbed emission $I_a(\Delta\lambda)$ integrated over wavelength. It was shown that

$$I_0 = \frac{\int_{-\infty}^{+\infty} I_a(\Delta\lambda)\, d(\Delta\lambda)}{W}, \tag{3}$$

where $W = 0.03$Å is the equivalent with of absorption of the hydrogen cell with $\tau = 10$, and $\Delta\lambda = \lambda_0 (V_D/c)$ is the Doppler shift, variable with the angular scanning. In practice the integral on $I_a(\Delta\lambda)$ is limited to a range $(-\Delta\lambda_m, +\Delta\lambda_m)$ provided by the Doppler scan instead of the theoretical infinite limits, with $\Delta\lambda_m = \lambda_0 V_{PT}/c$ (V_{PT} is the projection of the relative velocity vector V_R on the scan plane P). Thus V_{PT} has to be large enough in order to reach Doppler shifts corresponding to vanishing absorption $I_a(\lambda)$. This is the reason why calculations were made only for the two scan planes P_4 and P_5 providing both a complete scanning of the line profile.

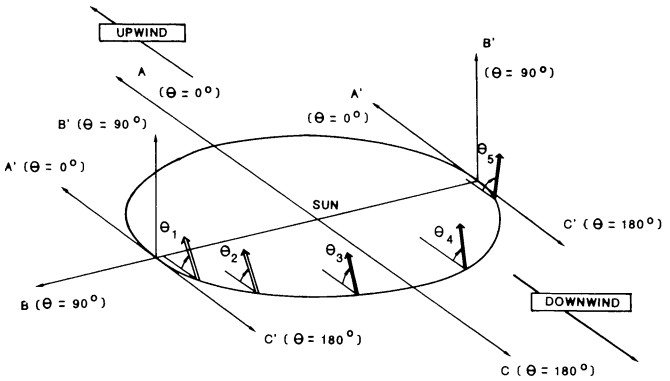

Fig. 10. The 5 lines of sight of maximum absorption are shown, together with the corresponding angles θ_i with the UPWIND direction. The geometry for the theoretical calculations of Wu and Judge (1980) which we use in Fig. 11 is also shown. Axis A, B, C and A', B', C', correspond to radial and non-radial directions respectively with values of θ equal to 0.90 and 180°. For simplicity, and only for the figure, V_w has been assumed to be in the ecliptic plane

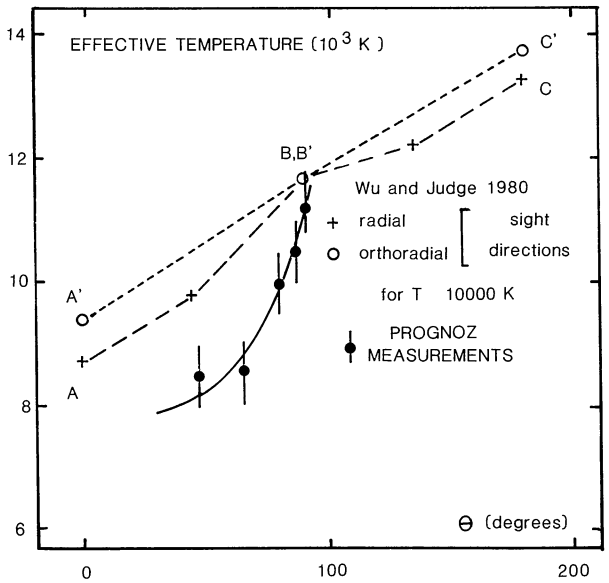

Fig. 11. The measured temperatures are plotted as a function of the angle θ with the UPWIND direction. Although our measurements cover a quite small interval of $\theta (\simeq 45°)$ it is large enough to observe an increase of the effective temperature with angle θ. However, the variation with θ is different from the theoretical calculation of Wu and Judge (1980) for radial (dashed lines) or non-radial (dotted lines) directions. The measured effective temperature increases towards the downwind direction more rapidly than predicted by Wu and Judge. Possible explanations are discussed in the text

In order to properly integrate the integral in (3), one has to know the velocity vector V_R, or rather its projection V_{PT} on the plane of observation, which would require in turn an exact knowledge of V_w. Though there is still some uncertainty on V_w, we were able to use expression (3) to derive an estimate of I_0, and an estimate $I_g = I_m - I_0$. Only an upper limit of $I_g \leqq 15$ Rayleigh was derived. When reported in the diagram of Fig. 9, it yields a lower limit of the effective temperatures of the interstellar hydrogen of $(7500 \pm 500$ K) in the solar system, and a lower limit of the span of effective temperature ob about 2400 K according to Fig. 9.

4. Discussion

In their 1977 paper previously quoted, Cazes and Emerich deduced from their data that the interplanetary profile was strongly assymmetric. Our data does not show such an effect, as can be seen in Figs. 2 to 6 where the curves $R(\phi)$ are quite symmetrical, and which are very near (except for a reversal of sign) the original spectral profile, as it is shown in Paper 1 when the optical thickness is only 10. It can also be remarked that the theoretical calculations of Wu and Judge (1980) do not show either this assymmetry effect. It should be reminded that for D2-A observations, the signal to noise ratio was not very large, and the contamination by the geocorona was rather large.

In Fig. 10 are represented schematically the positions and the directions in which were measured the effective temperatures T_e, with respect to the mean velocity vector V_w. We have indicated the angles θ_1 to θ_5 between the lines of sight S_1 to S_5 where T_e was measured, and the velocity vector V_w. Here, instead of using the present determination of V_w we have used a more accurate determination of V_w done with the observations of the helium focusing cone (Dalaudier et al., 1984), with $\lambda_w = 74.5 \pm 3$ and $\beta_w = -6 \pm 3°$ in ecliptic coordinates. (In fact the following results do not change if another value of V_w inside the interval founded in Sect. 2 is used.) As it is known, the solar environment, in general, increases the apparent temperature T_e with respect to the LISM temperature T, and the increase is larger in the downwind region of the solar system. In Fig. 10 are also represented the lines of sight corresponding to the line profile calculations of Wu and Judge (1980). Lines A, B, C are radial lines of sight, whereas lines A', B', C' are starting from a point of the earth's orbit at $\lambda = \lambda_w - 90°$. A comparison between these theoretical results and our measurements is shown on Fig. 11, which is a plot of T_e as a function of θ. Calculations by Wu and Judge where made for $T = 10{,}000$ K. Except for a small range of low values of $\theta \leqq 30°$, T_e is larger than T in their calculations.

Though the two geometries (theoretical and actual), do not coïncide exactly they are not very different and a comparison can be made. Data points $T_e(\theta_i)$ show that indeed there is an increase of the effective temperature T_e with θ, as expected from the theoretical calculations of Wu and Judge. It can be remarked that the temperature measured at S_5, $T_e = 11{,}300$ K at the point where θ is maximum ($\theta_5 = 89°$), is larger than the temperature $T_e = 10{,}500$ K measured at S_5 ($\theta_4 = 86°$), though the position S_4 is more downwind than the position S_5. It means that the direction of observation is more important than the position of the observer to yield the heating effect $T_e - T$.

This is simply due to the fact that the differences of 0.5 UA for positions are smaller than the region from which the observed interplanetary emission is generated, which ranges over several UA. Comparing now with our measurements, it appears that the effective temperatures evolve in a very different way from the model prediction. The rate of increase becomes greater as θ increases instead of being nearly constant according to the model.

One possible explanation is that the set of parameters (T, μ and ionization parameters) used by Wu and Judge could be sufficiently different from the exact values to explain the observed differences. On the other hand they could also show the presence of another effect inside the ionization cavity, as for example a strong heating by solar protons and electrons. The possibility of an increase of linewidth by multiple scattering is also not completely precluded (Holzer, 1977; Keller et al., 1981). However, it appears now that an extensive discussion of this difference would require to compute line profile models for many sets of parameters and many lines of

sight. At any rate, according to the model and data evolution in Fig. 11, we can evaluate the temperature T at infinity in the range $T \simeq 8000 \pm 1000$ K, by extrapolating back to $\theta \simeq 60°$, where in the model $T(60°) \simeq T$ at infinity.

5. Conclusion

Measurements of the interplanetary Ly α line profile were performed at various places in the solar system with the Doppler angular scanning method. The geometrical method established in paper 1 to analyze the results yielded the following findings:

– a first estimate of the position of V_w was determined to be:

$\lambda_w = 253°$ to $281°$

$\beta_w = 9°$ to $24°$

$V_w = 17.5$ to $25.4\,\mathrm{km\,s^{-1}}$

which compares fairly well with other determinations derived by other methods and authors:

– $\lambda_w = 265°$, $\beta_w = +8°5$, (Bertaux and Blamont, 1971)

– $V_w = (22 \pm 3)\,\mathrm{km\,s^{-1}}$ (Adams and Frisch, 1977)

– $\lambda_w = (253 \pm 3)°$, $\beta_w = (4 \pm 3)°$ Weller and Meier, 1981 (from Helium measurements)

– $\lambda_w = (254 \pm 3)°$, $\beta_w = (7 \pm 3)°$ Dalaudier et al., 1984 (from Helium measurements).

Our present determination is independent of the possible existence of a galactic background.

– It was demonstrated that the bulk velocity V of H atoms in the solar system is not same at all locations.

– An upper limit to a possible galactic background I_g of 15 Rayleigh was obtained (less than 5% of the maximum interplanetary emission). Whatever the value of I_g is, the effective temperature T_e observed in the solar system depends on the looking direction, and covers a range of 2500–3000 K. The temperature T before interaction with the solar environment is evaluated $T = 8000 \pm 1000$ K.

Both the bulk velocity and the thermal spread (averaged along a line of sight) of the interstellar H atoms flowing in the solar system are for the first time observed to be influenced by the interaction with the Sun, the unbalance between solar gravitation and solar Ly α radiation pressure, ionization effects and perhaps additional heating effects.

All these effects can be modelled, and the result of this modelling will be presented in a future work. Curves of the intensity $I(\phi)$ and reduction factor $R(\phi)$ are modified from the simple uniform gaussian case. Only a comparison of computed and observed curves will allow a more accurate determination of T and V_w. As a bonus, the exact value of μ and the ionization rate of H atoms by the sun can be derived from this comparison, two parameters which can be of interest to the solar physicists.

Acknowledgements. We wish to thank Jean Francis Brun, who acted as Project Manager for the construction of this experiment, Jean Claude Lebrun, for assistance on the computing system CYBER, kindly provided by Centre National d'Etudes Spatiales, and Mr. Pokras for data reduction at IKI (Space Research Institute in Moscow).

Refernces

Adams, T.F., Frisch, P.C.: 1977, *Astrophys. J.* **212,** 300
Bertaux, J.L., Blamont, J.E.: 1971, *Astron. Astrophys.* **11,** 200
Bertaux, J.L., Ammar, A., Blamont, J.E.: 1972, *Space Res.* **12,** 1559
Bertaux, J.L., Lallement, R.: 1984, *Astron. Astrophys.* **140,** 230
Bertaux, J.L., Blamont, J.E., Mironova, E.N., Kurt, V.G., Bourgin, M.C.: 1977, *Nature* **270,** 156
Cazes, S., Emerich, C.: 1977, *Astron. Astrophys.* **59,** 59
Dalaudier, F., Bertaux, J.L., Kurt, V.G., Mironova, E.N.: 1984, *Astron. Astrophys.* **134,** 171
Fahr, H.J.: 1974, *Space Sci. Rev.* **15,** 483
Fahr, H.J.: 1978, *Astron. Astrophys.* **66,** 103
Holzer, T.E.: 1977, *Rev. Geophys. Space Phys.* **15,** 467
Keller, H.U., Richter, K., Thomas, G.E.: 1981, *Astron. Astrophys.* **102,** 415
Kunc, J.A., Wu, F.M., Judge, D.L.: 1983, *Planetary Space Sci.* **31,** 1157
Thomas, G.E.: 1972, Solar wind NASA SP 308
Thomas, G.E., Blamont, J.E.: 1976, *Astron. Astrophys.* **51,** 283
Weller, C.S., Meier, R.R.: 1981, *Astrophys. J.* **246,** 386
Wu, F.M., Judge, D.L.: 1978, *Astrophys. J.* **225,** 1045
Wu, F.M., Judge, D.L.: 1979, *Astrophys. J.* **231,** 594
Wu, F.M., Judge, D.L.: 1980, *Astrophys. J.* **239,** 389